Comparison of Magnetic Field and AC Losses in Solenoid Coil and Pancake Coil with HTS tape

Myungjin Park, Kwangyoun Lee, Jungwook Sim, Gueesoo Cha, Jikwang Lee*

Dept. of Electrical Eng., Soonchunhyang University, Shinchang, Asan, Choongnam, Korea

* Dept. of Electrical Eng., Woosuk University, Woosuk University, Wanjoo, Chunbuk, Korea

pj1973@hanmail.net

Abstract-- When HTS tapes are used in power application, they are used by winding form, such as, a pancake and a solenoid.

When AC current is applied to the coil, Ac magnetic field is generated in winding. This AC magnetic field acts as an external magnetic field and makes loss. In this paper, the radial magnetic field component (B_r) and the axial magnetic field component (B_z) in a pancake and a solenoid were calculated by numerical analysis method and compare with measured value. AC losses of a short sample were calculated by Norris equation and a numerical analysis based on Brandt equation. AC losses of the pancake coil and the solenoid coil were also calculated.

1. INTRODUCTION

Bi-2223 tapes have been developed for power application, such as, HTS transformers, HTS current limiter and HTS power transmission cable. HTS tape is wound as a coil shape in those applications. Loss by adjacent coils is generated when AC current is applied to the coil. In general, it is important to estimate magnetic field that is applied HTS tape because critical current I_c of HTS tape and loss depend on external magnetic field. Also it is one of important parts in application of HTS tape.

In this paper, magnetic fields of two models were numerically calculated, the first model was a pancake type that consisted of 6 single-pancakes and the second model was solenoid type. The same current was applied the two models to compare magnetic distributions. The radial magnetic field component (B_r) and the axial magnetic field component (B_z) were measured under the same conditions. Measured values were compared with calculated values by numerical analysis. AC losses were calculated by using magnetic field that were generated in HTS tape.

2. SOLENOID WINDING AND PANCAKE WINDING

Characteristics of Bi-2223 used in this paper are presented table I. One pancake type winding and one solenoid type winding were manufactured for experiment. The pancake winding consisted of 6 single-pancakes.

Diameter of each single-pancake was 100mm and number of turn was. There was a groove to measure the radial magnetic field component (B_r) and the axial magnetic field component (B_z) in the vicinity of the inner surface of coil.

TABLE I
Specification of Bi-2223

Thickness of tape	0.203(mm)
Thickness of core	0.15(mm)
Width of tape	4.1(mm)
Width of core	3.7(mm)
J_e	>12kA/cm^2
I_c	>100A
Max. stress(77k)	85Mpa
Max. strain	0.15%
Min. Bend Diameter	100mm

Total number of turns in the pancake winding were 36 and its height was 76mm. Distance between each pancake was 10.4mm.

A solenoid that has 4 layers and 36 turns was manufactured to compare B_r and B_z with that of the pancake winding. HTS tape was wound from first layer to fourth layer continuously. Height of the solenoid was 76mm and a gap between turns was 4mm. To insulate each layer, an insulation tape of 0.2mm thickness was used. 50A DC currents were applied to both models.

Two Hall probes were used to measure B_r and B_z of models. B_r and B_z were measured at the same time. r and z indicate perpendicular and parallel direction to HTS tape surface respectively. Magnetic field B_r and B_z were measured in the vicinity of inner surface of the models. The Hall probe moved parallel with coil axis and radial direction. Table II and Fig.1 show the specifications and shape of models.

<div style="column: left">

TABLE II

Specification of models

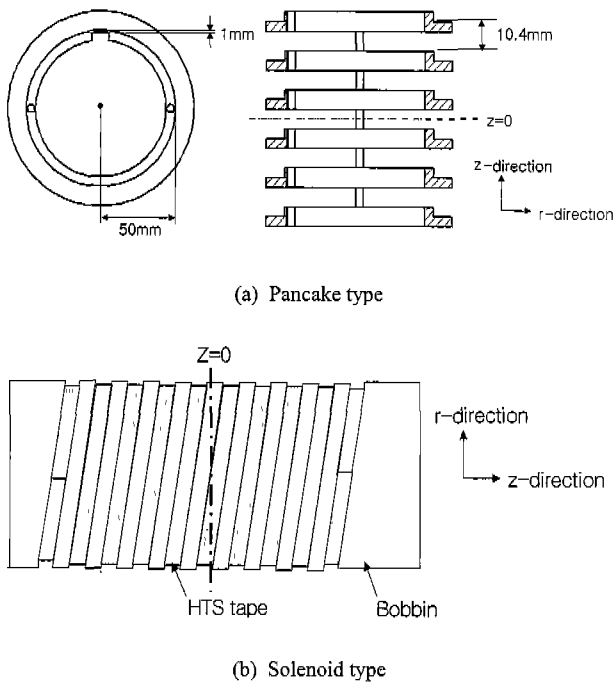|	Pancake	Solenoid
Gap of interturn	10.4mm	4mm
Height	76mm	76mm
Number of turns	36	36
Gap between layer	0.2mm	0.2mm
Diameter	100mm	100mm
Total length of tape	11.45m	11.45m

(a) Pancake type

(b) Solenoid type

Fig. 1. Schematics of models.

In this paper, magnetic fields of models were calculated by numerical analysis method before experiment. All conditions of the analysis method were same with experiment. A spiral conductor was designed to describe a spiral winding of solenoid coil in this simulation.

3. MAGNETIC FIELD DISTRIBUTION

Fig.2 presents the radial magnetic field (B_r) of the pancake coil at radial distance r=49mm and 48.35mm from center. The measured values show good agreement with calculated values. Distribution of B_r presents the teeth of a saw. HTS tapes are placed z=5.2~9.2mm, 19.6~23.6mm and 34~38mm. Maximum value of calculated and measured B_r are 0.0177 and 0.0151T respectively at r=49mm, z=39mm and 40.3mm. The closer to the end of pancake winding, magnitude of B_r was increased. Also B_r in end of tape was bigger then that of the center of tape.

</div>

<div style="column: right">

Fig.3 presents the axial magnetic field component (B_z) of the pancake coil at radial distance r=42mm and 41.35mm from center. Distribution of B_z presents nearly the same as a sinusoidal curve. Maximum value of calculated and measured B_r is 0.0191 and 0.0245 T respectively at r=42, z=7.6 and 7mm. B_z increases from the center of gap to center of tape and decreases to next center of gap with increasing z.

Fig.4 and Fig.5 present B_r and B_z of the solenoid model. Because of the gap interturn, B_r had distribution of the weak the teeth of a saw in Fig.4. It shows a difference in conventional magnetic fields of numerical calculation in 2D. When the second layer of solenoid is wound, HTS tape is overlapped upon the first layer. The third and fourth layers are wound at the same position with the first and second layer respectively. Because B_r is reduced at the overlapped part, the change of amplitude of B_r is small. Fig.5 presents B_z of solenoid. With increasing z, B_z decreases. Although the gap is 4mm, it does not present a sinusoidal curve as pancake B_z because of the overlapped parts of interlayers.
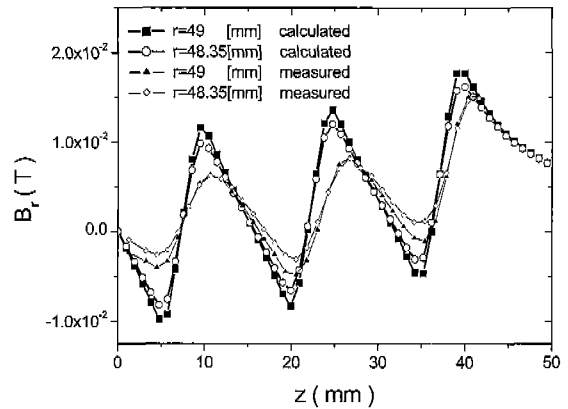

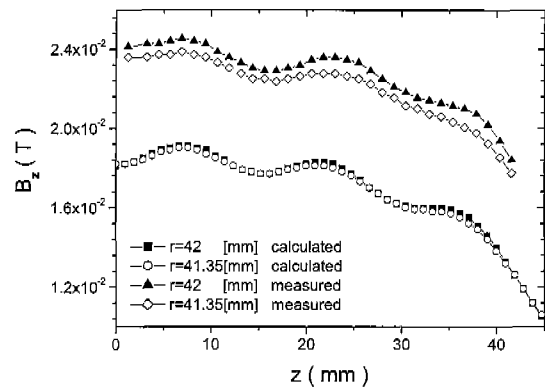Fig. 2. The radial magnetic field distribution of the pancake.

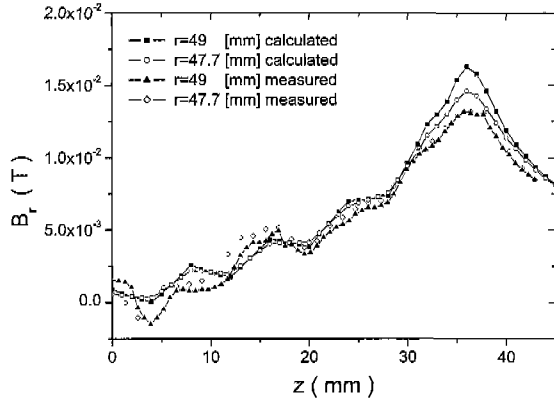Fig. 3. The axial magnetic field distribution of the pancake.

</div>

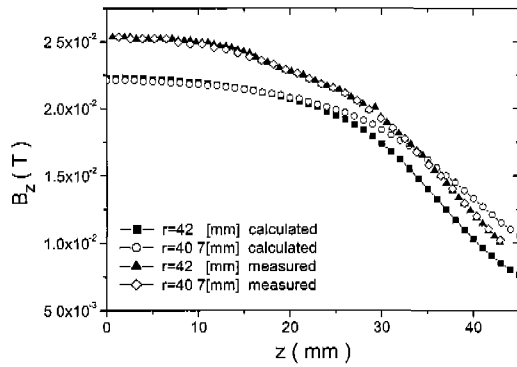Fig. 4. The radial magnetic field distribution of the solenoid.

Fig. 5. The axial magnetic field distribution of the solenoid.

4. CALCULATION OF AC LOSS

Transport-current loss is the power that is delivered by the power supply that enables the transport current I to flow through the conductor. The voltage along the sample is a measure for the dissipated power.

The magnetization loss is the power that is dissipated in the conductor when an alternating magnetic field B is applied to the conductor. The energy is delivered by the power supply of the magnet. The magnetic moment m of the sample provides the information about the amount of energy that is dissipated from the magnetic field. [4]

4.1. Self-field Loss

Transport-current in a superconductor generates a magnetic self-field around the conductor. During each current cycle the self-field partially penetrates the superconductor and therefore cause a hysteresis type loss that called the (self-field) transport current loss. If there is no alternating magnetic field other then the self-field, the loss per cycle per volume in a superconductor with an elliptical cross-section is [1]

$$P(F) = \left(\frac{\mu_0 I_c^2}{\pi}\right)\left[(1-F)\ln(1-F)+(2-F)\frac{F}{2}\right]$$

$$(\text{J/m/cycle}) \quad (1)$$

where $F=Ic/Ip$, Ic is critical current and Ip is a peak value of applied AC current.

Fig.6 presents the self-field loss by equation (1) and measured self-field loss. Measured values show good agreement with Norris equation over the whole range.

4.2. Magnetization Loss

Magnetization loss is classified by direction of external field that applied to cross-section of HTS tape. Fig.7 presents magnetic field of parallel, perpendicular and an arbitrary incident angle. In general, equation (2) and equation (3) are adapted to calculate losses for the parallel and the perpendicular field, respectively.
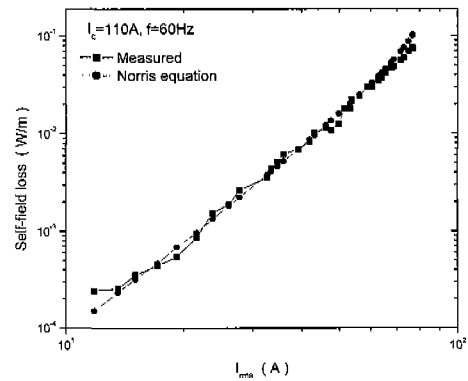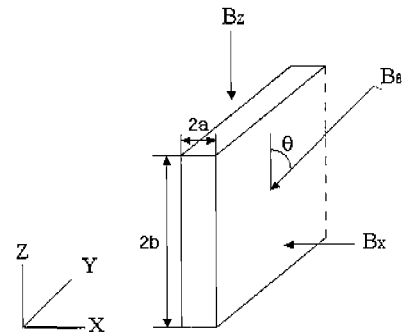

Fig. 6. Self-field losses by Norris equation and measurement.

Fig. 7. Magnetic field orientation B_x, B_z and B_θ are a perpendicular, a parallel and an incident magnetic field respectively.

$$P_{//} = \frac{2fB_P^2}{\mu_0}\beta_{//}^3 \qquad B < B_p$$

$$= \frac{2fB_P^2}{\mu_0}(\beta_{//}^3 - \frac{2}{3}) \quad B > B_p \qquad (J/m^3) \qquad (2)$$

where B_p is the field of full penetration and $\beta_{//} = B/B_p$. B is external magnetic field that applied parallel to cross-section of HTS tape.

$$P_\perp = K\frac{4\pi a^2 f}{\mu_0}B_cB\left[\frac{2}{\beta_\perp}\ln(\cosh\beta_\perp) - \tanh\beta_\perp\right]$$

$$(J/m) \qquad (3)$$

where $\beta_\perp = \dfrac{B}{B_c}$, $B_c = \dfrac{2\mu_0 J_c b}{\pi}$ and B is external

magnetic field applied to perpendicular to HTS tape. K is a geometrical parameter to take into account the shape of the HTS tape. [2]

Fig.8 shows measured and calculated losses for parallel external magnetic field. Fig.9 shows magnetization loops of the HTS tape in parallel magnetic field.

4.3.   Numerical Calculation

Transport-current in a superconductor generates a magnetic self-field around the conductor and self-field by transport current causes a hysteresis type loss. Fig.10(a) shows the magnetic fields distribution inside HTS tape with rectangular cross-section when current flows through HTS tape. On the other hand, if magnetic fields are presents as Fig.10(b) in free space and HTS tape are placed as Fig.10(c), loss by these magnetic field is generated. Also the loss in Fig.10(c) will be approximated to transport current loss by Norris equation because this loss is a hysteresis type loss by self-field.

In numerical calculation, magnetic fields inside the HTS tape were calculated by using Finite Element Analysis and the equation (2) and (3) were employed. Equation (4) was used for magnetic field that applied to cross-section of HTS tape with an arbitrary incident angle.

$$P(B) = P_{//}(B_{//}) + P_\perp(B_\perp) \qquad (4)$$

where B is magnetic field that applied to cross-section of HTS tape with an arbitrary incident angle, $B_{//} = B\sin\theta$ and $B_\perp = B\cos\theta$.

(a)   Flux density in HTS tape.

(b) Magnetic fields in HTS tape.   (c) Magnetic fields in free space.

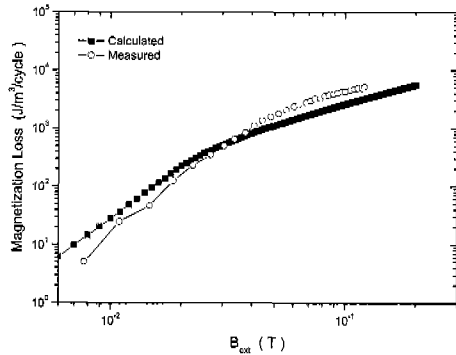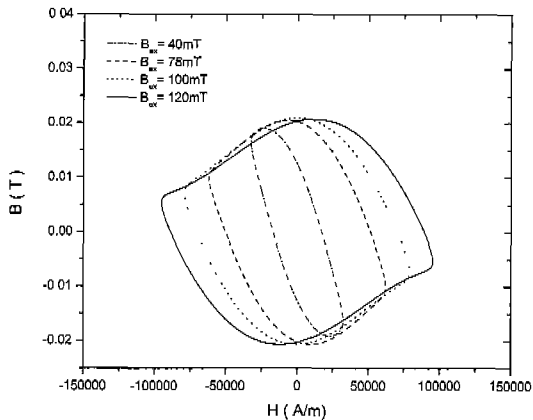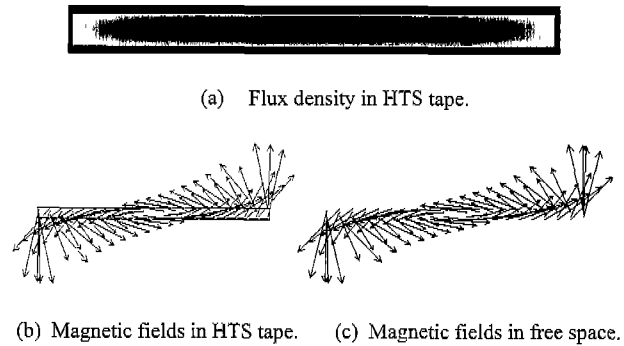Fig. 10. Flux density and magnetic field in HTS tape.

Fig. 8.   Comparison of measured and calculated losses for parallel external magnetic field.

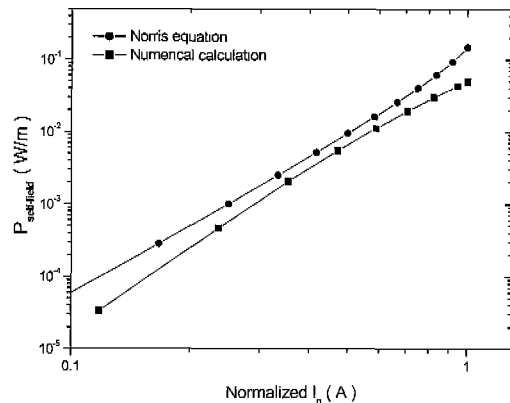Fig. 9. Magnetization loops of HTS tape in parallel magnetic field.

Fig.11. Comparison of self-field loss by Norris equation and numerical calculation.

Fig.11 presents losses of Norris and numerical calculation. The normalized current $I_n=I_c/I_p$ and geometrical parameter $K=1$ in equation (3).

4.4.   AC losses of the pancake and the solenoid

Losses of the pancake and the solenoid have been calculated by using above numerical calculation. The solenoid was considered as a symmetrical geometry in 2D. Average I_c of the six pancakes winding were 80A and Ic of the solenoid was 61A.
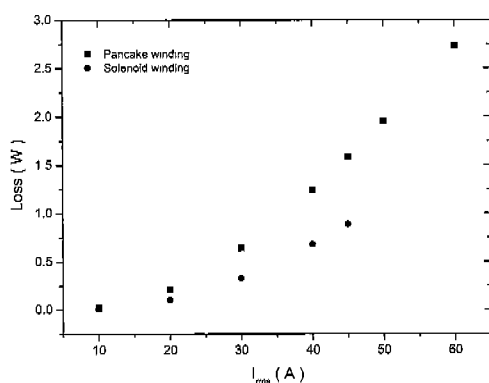

Fig.12. Losses of the pancake and the solenoid winding.

Fig.12 presents calculated losses of both models in AC currents. Losses of the pancake and solenoid winding are 0.64 and 0.33 (W) respectively in 30A (rms). Losses of pancake are about 2 times bigger than that of the solenoid over the whole ranges. It indicates that losses in HTS tape are greatly influenced by magnetic field distribution.

5.   CONCLUSION

In this paper, the radial magnetic field B_r and the axial magnetic field B_z were calculated and measured for the pancake and the solenoid model. Also losses by magnetic fields in the pancake and the solenoid were calculated and compared in numerical calculation. Losses of pancake are about 2 times bigger than that of the solenoid over the whole ranges.

The difference in Fig.11 seems that magnetization losses by equation (2) and (3) differ from measured losses but Norris equation shows good agreement with measured data in Fig.6. Magnetization loss also depends on geometrical shapes of HTS tape.

It needs more data to get more accurate calculation results, such as, geometrical parameter K and magnetization loss of HTS tape for magnetic field with an arbitrary incident angle.

REFERENCES

[1]   Oomen, Marijn Pieter, AC loss in superconductor tapes and cables, Twente University, 2000.
[2]   A. Wolfbrandt, N. Magnusson and S. Hornfeldt, "AC loss in a BSCCO/Ag Tape Carrying AC Transport Currents in AC Magnetic Fields Applied in Different Orientations", IEEE Transactions on Applied superconductivity , Vol. 11. 4, No.4, pp. 4123-4127. 2001.
[3]   M. Polak, P. Usak, J. Pitel, L. Jansak, Z. Timoransky, F. Zizek, H. Piel, "Comparison of Solenoidal and Pancake Model Windings for a Superconducting Transformer", IEEE Transactions on Applied superconductivity, Vol.11, No. 1, pp. 1478-1481, 2001.
[4]   Jacob Johan Rabbers, AC loss in superconducting tapes and coils, Twente University, 2001.